

Supporting Information

Molecular Scaffolding Strategy with Synergistic Active Centers to Facilitate Electrocatalytic CO₂ Reduction to Hydrocarbon/Alcohol

Yan Jiao^{1,‡}, Yao Zheng^{1,‡}, Ping Chen^{1,2,‡}, Mietek Jaroniec,³ Shi-Zhang Qiao^{1,4*}

¹ *School of Chemical Engineering, The University of Adelaide, Adelaide, South Australia 5005, Australia*

² *School of Chemistry and Chemical Engineering, Anhui University, Hefei, P. R. China*

³ *Department of Chemistry and Biochemistry, Kent State University, Kent, Ohio 44242, USA*

⁴ *School of Materials Science and Engineering, Tianjin University, Tianjin 300072, China*

This PDF file includes:

Computational Section

- Free Energy Computation
- Reaction Intermediates
- Reaction Free Energy Diagrams

Experimental Section

- Characterization of Catalysts
- Electrochemical Measurements

Figures S1 to S7

Tables S1 to S5

Reference 1-6

Free Energy Calculation

Free energies of each state are obtained by

$$G = E + \text{ZPE} + \int C_p dT - TS \quad (\text{Eq. 1})$$

where zero point energies (ZPE), enthalpic temperature correction ($\int C_p dT$) and entropy correction (TS) were calculated on the basis of vibration analysis obtained by standard methods and used to convert the electronic energies into free energies at 298.15 K (Table S2); gas-phase free energies were obtained by standard methods as well (Table S3).¹ Our computed equilibrium potentials for several critical products agree well with experimental observations (Table S4).² During the vibration analysis for intermediate states, frequencies were calculated by treating all 3N degrees of the adsorbates as vibrational in the harmonic oscillator approximation, and assuming that any changes in the vibrations of the substrate surface were minimal, in accordance with previous publications.³ The standard state pressure of 101,325 Pa was used for the fugacity of gaseous species (CO₂, CO, CH₄); while a fugacity of 3534 Pa, 19 Pa and 3242.4 Pa were used for H₂O, HCOOH, and C₂H₅OH, respectively, corresponding to vapour pressure of water, 1M HCOOH.⁴ The adsorbate solvation effects were included approximately in the same manner as in previous studies: hydroxyl adsorbates (*OH) and hydroxyl functional groups (*R-OH) were stabilized by 0.50 eV, and 0.25 eV, respectively, and intermediates containing adsorbed CO such as *CO and *CHO were stabilized by 0.10 eV.^{3a, 4} Gas phase energetics of species containing a CO backbone were compensated to match experimental values, to be specific, 0.19 eV compensation for CO₂, -0.30 eV for CO, and 0.15 eV compensation for HCOOH.

The computational hydrogen electrode (CHE) model was applied to include the electrode potential correction to the free energy of each state, by considering the electrochemical proton-electron transfer being a function of the applied electrical potential.⁵ In this model, the free energy of a proton-electron pair at 0V *vs* RHE is defined to be equal to ½ of the H₂ free energy at 101,325 Pa. The free energy of each intermediate, calculated at 298.15 K, is then a function of the electrode potential (U) according to

$$G(U) = G(0V) - neU \quad (\text{Eq. 2})$$

where e is the elementary charge of an electron, n is the number of proton-electron pairs transferred to the investigated intermediate or final states. The application of Eq.2 to an elementary reaction pathway results in the electrode potential corrected free energy pathway, therefore provides a venue to evaluate at which potential a certain CO₂ electroreduction pathway opens, as well as defining the potential dependent reaction step. In the current study, the relative free energies of the reaction intermediates were taken only as an indication the starting point of different pathways in the electroreduction of CO₂, since reaction

barriers were not considered. As indicated in earlier studies, barriers for proton transfer to adsorbates from solution are normally low enough to be surmountable at room temperatures.⁶

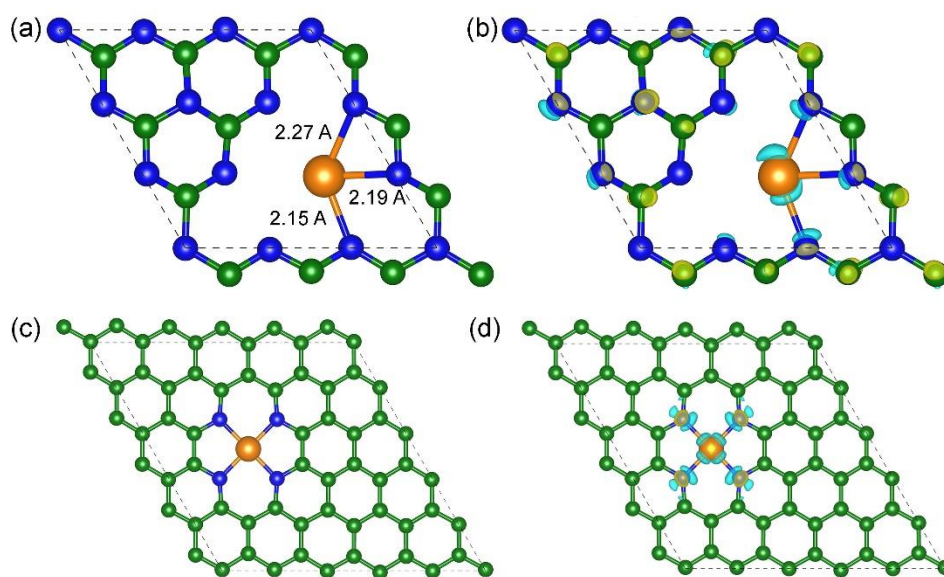


Figure S1 (a) Optimized geometry and (b) charge density difference for Cu-C₃N₄. (c) Optimized geometry and (d) charge density difference for Cu-NC. Color code: blue, nitrogen; green, carbon; gold, copper. Unit for charge density difference is 0.01 e/Bohr³, yellow indicates electron accumulation, and cyan indicates electron depletion.

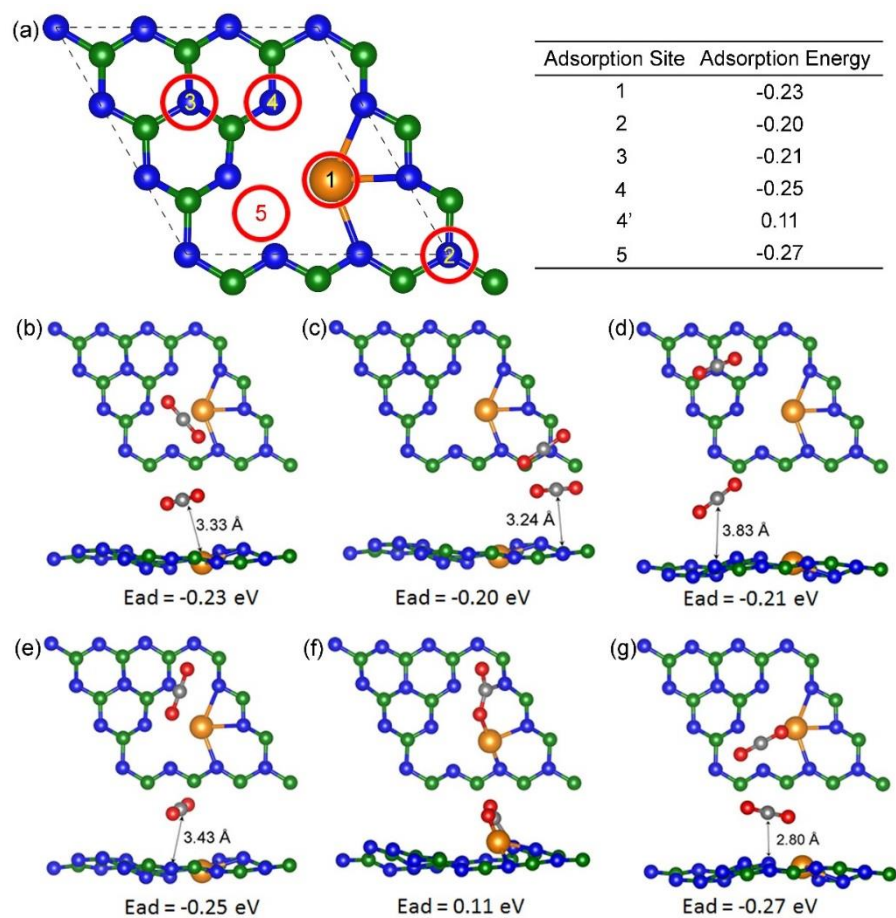


Figure S2 (a) CO₂ adsorption summary on Cu-C₃N₄. Red circle indicates the adsorption sites that have been considered in this study. The adsorption energy for each site is shown in the table. The corresponding configurations are shown in (b) – (g). Color code: blue, nitrogen; green, carbon on Cu-C₃N₄; gold, copper; grey, carbon on CO₂; red, oxygen.

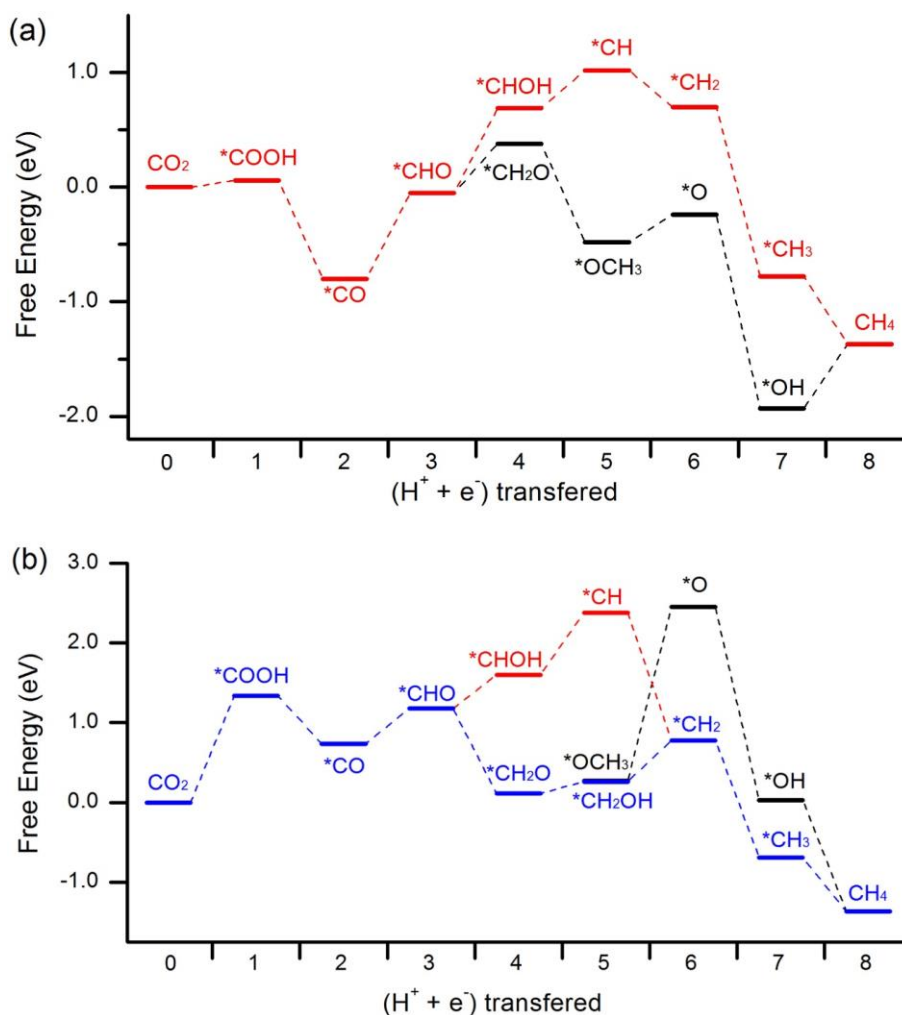


Figure S3 Comparison of reduction pathways for methane production on (a) Cu-C₃N₄ and (b) Cu-NC. Black lines follow the set of reaction intermediates that lead to the lowest possible reaction pathway for the Cu-C₃N₄ surface (as presented in Figure 1 of the manuscript), red lines follow the reaction pathway discussed in reference 9f, and blue line in (b) indicates the lowest possible pathway on Cu-NC.

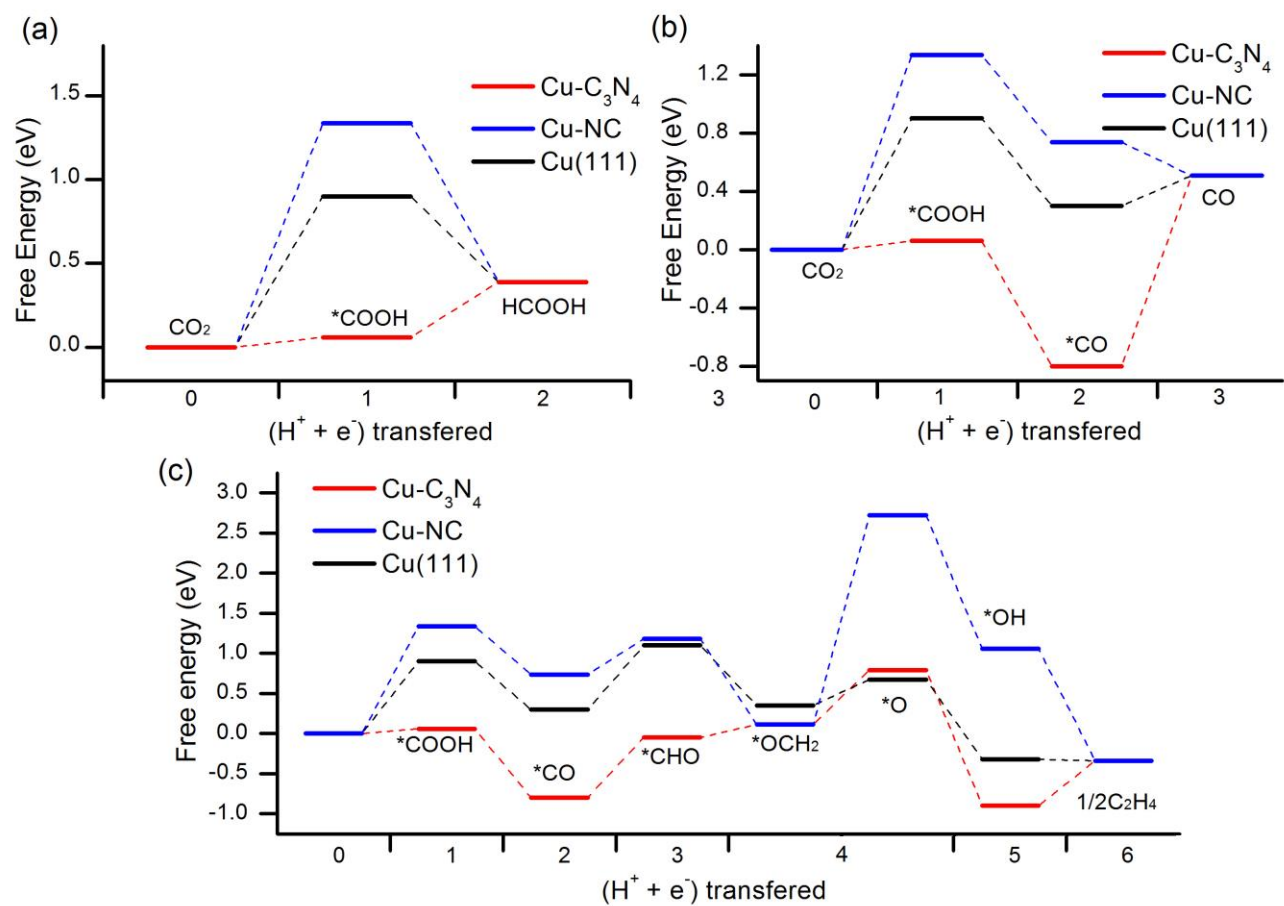


Figure S4 Pathways of CO₂ reduction to HCOOH, CO, and C₂H₄. Different to other products, C₂H₄ as shown in (c) is a C₂ product, and the pathway shown here is a ‘half reaction’ that includes six electron/proton pair transfers.

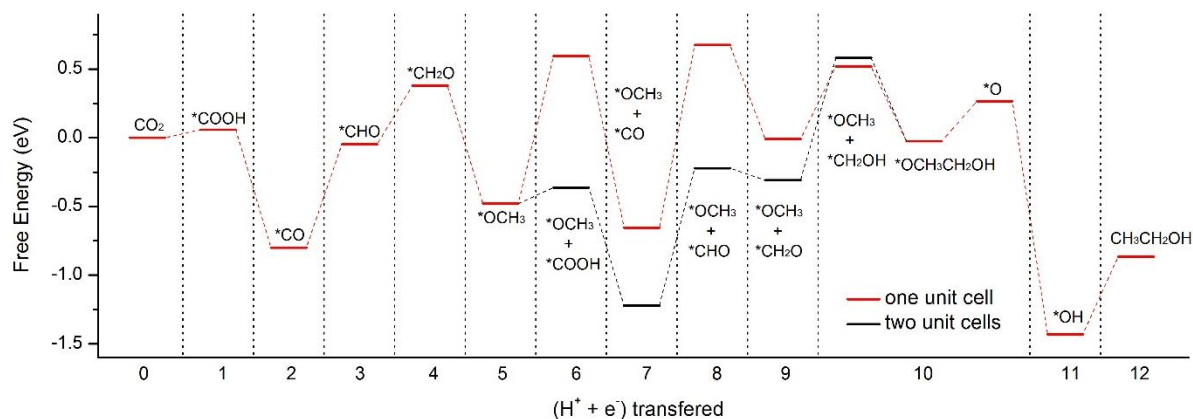


Figure S5 Free energy diagram of CO₂ reduction to CH₃CH₂OH on Cu-C₃N₄.

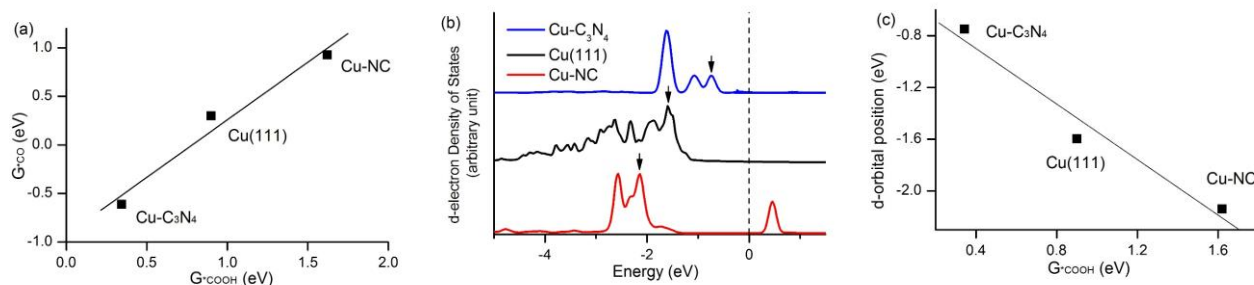


Figure S6 (a) Relationship between *COOH with *CO adsorption on three surfaces. (b) Projected d-orbital DOS (PDOS) on Cu atom of Cu-C₃N₄, Cu(111) slab and Cu-NC, dashed line indicates Fermi level. (c) The relationship between Cu PDOS d-orbital peak position (the position of the first peak next to Fermi level).

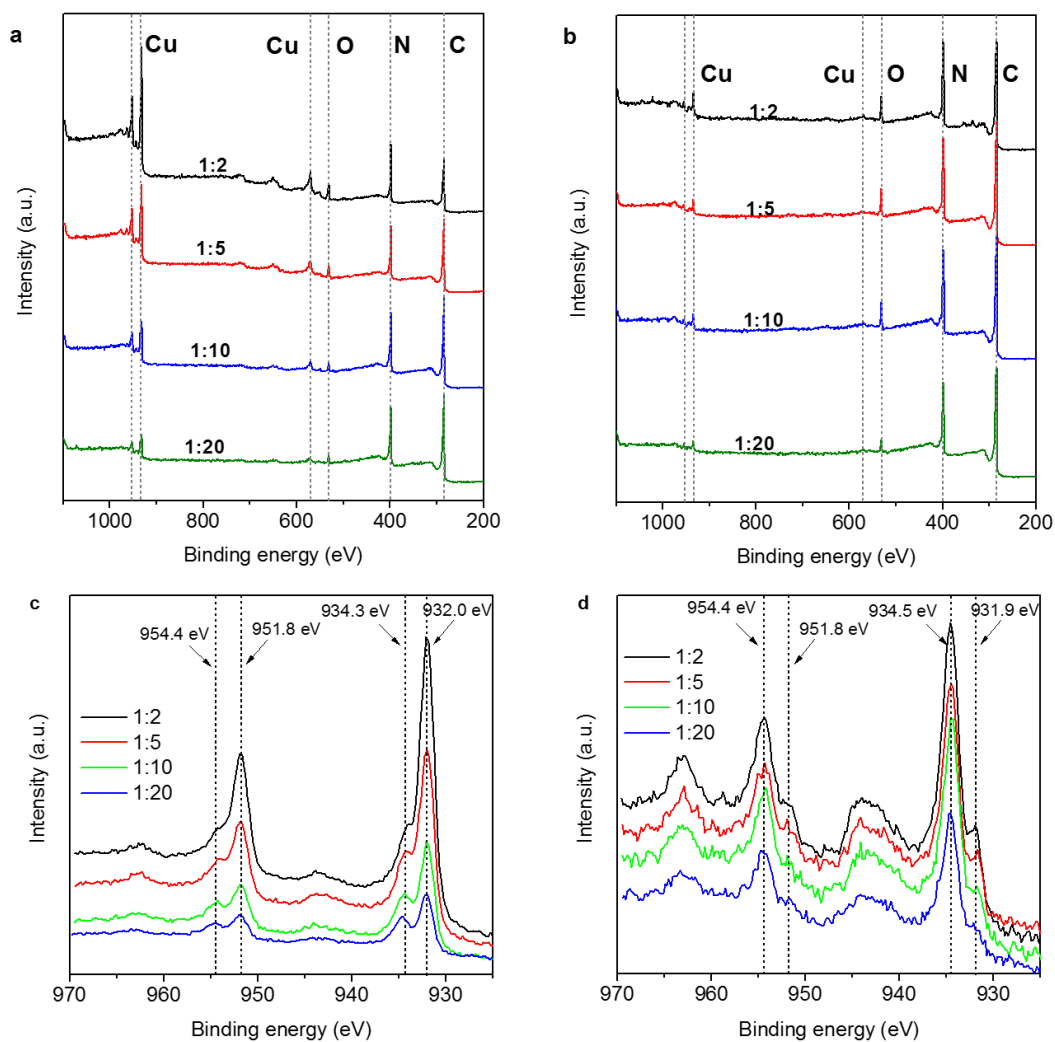
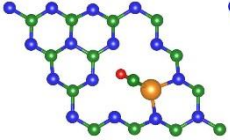
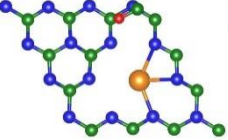
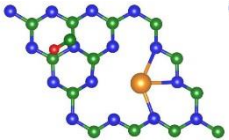
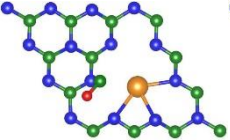
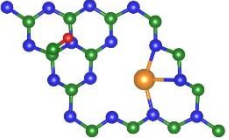
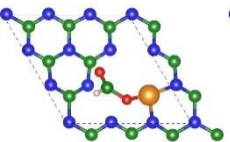
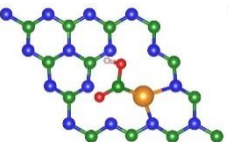
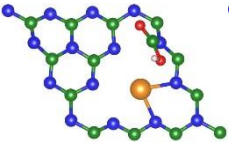
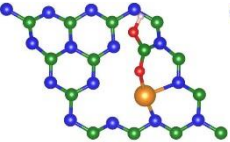
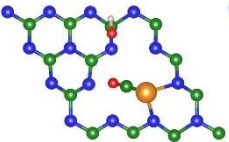
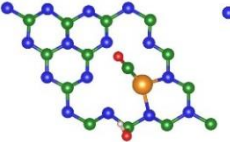
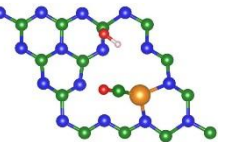
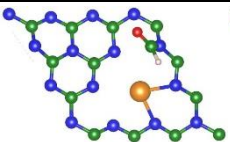
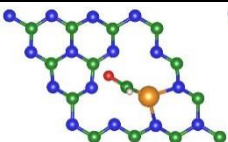
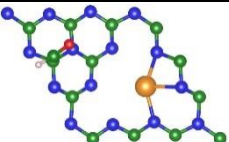
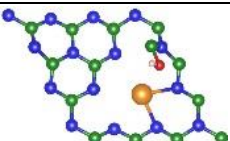
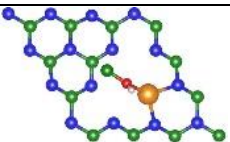
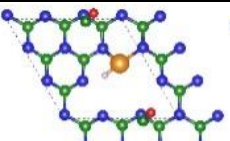
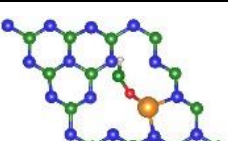
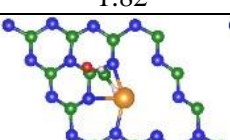
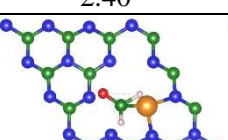
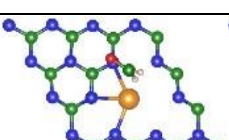
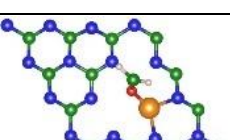
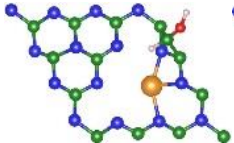
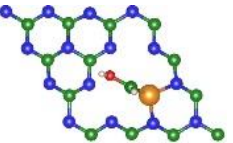
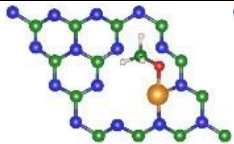
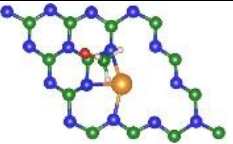
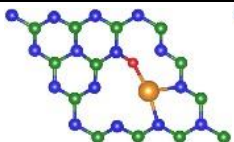
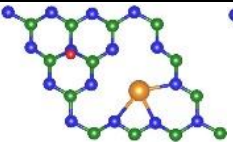
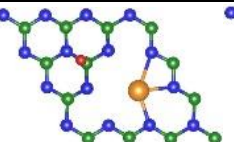
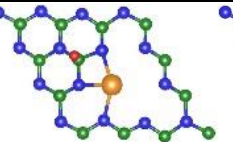
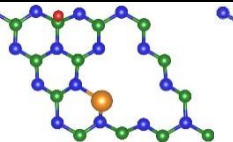
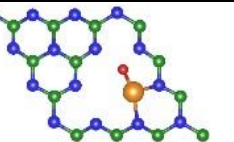
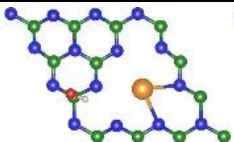
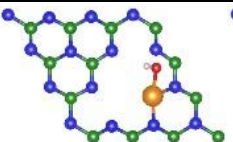
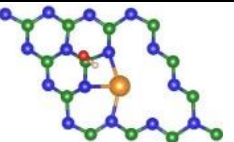
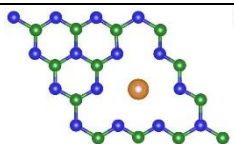
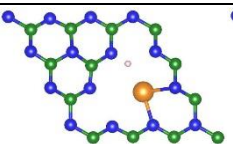
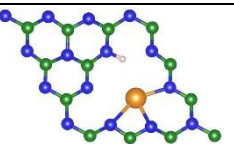
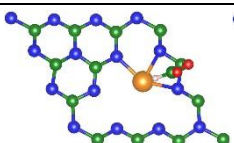
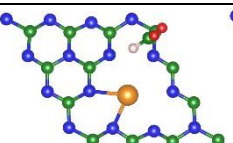
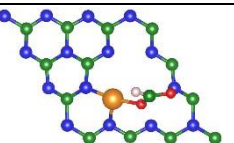
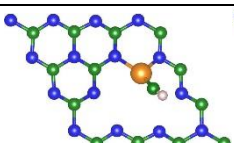
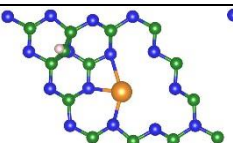
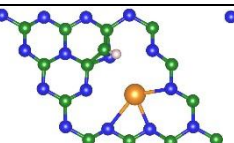
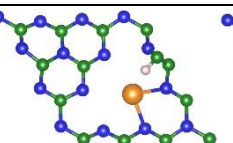
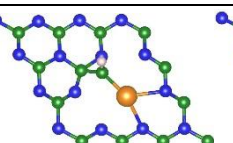
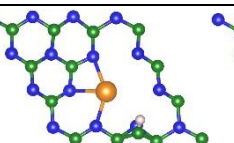
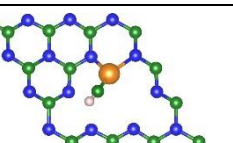


Figure S7 XPS survey spectra of different Cu-C₃N₄ samples before (a) and after (b) acid wash. High-resolution Cu 2p XPS spectra of different Cu-C₃N₄ samples before (c) and after (d) acid wash.

Table S1 Summary of energy and configurations of possible reaction intermediates on Cu-C₃N₄ explored by this study. Reported energies (eV) are referenced to the electronic energy of the clean Cu-C₃N₄ substrate with reference atom energies for H, C, and O obtained from ½ H₂, graphene, and (H₂O – H₂), respectively.

*CO	    
	0.27 1.83 1.82 1.80 2.55
*COOH	      
	0.21 0.92 1.79 1.86 0.51 0.49 0.29
*CHO	  
	1.60 1.01 0.76
*COH	
	3.34
*OHC	
	4.63
*OCH	 
	1.82 2.40
*OCH₂	   
	1.69 0.85 1.17 0.59

*CHOH	  1.78 1.16
*OCH₃	  -0.25 -0.40
*O	      2.24 3.70 1.58 1.17 1.28 2.22
*OH	   -0.04 -0.32 -0.26
*H	   0.77 0.17 0.12
*OCHO	   1.06 1.35 0.59
*CH	       3.20 3.79 1.86 2.83 1.99 1.86 3.20

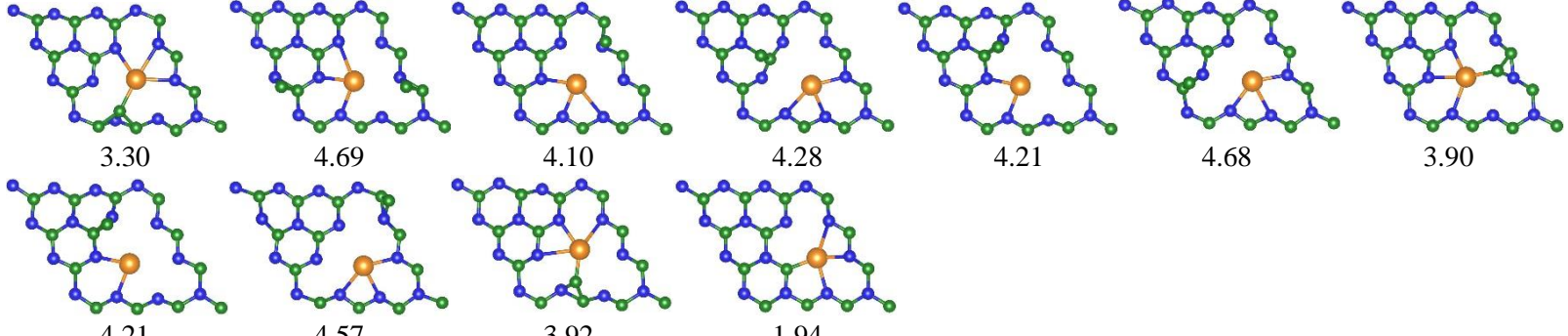
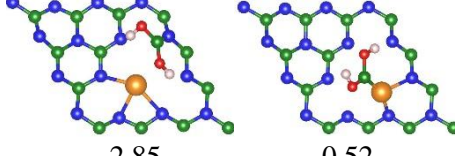
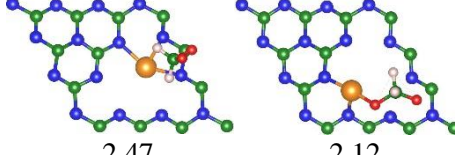
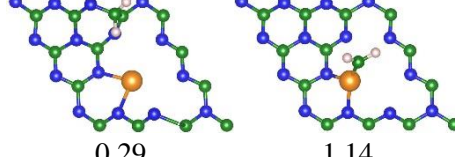
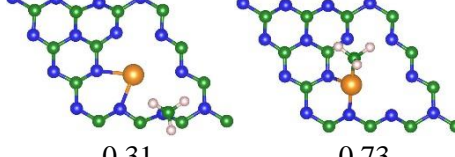
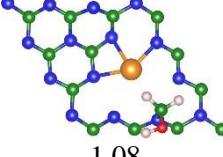
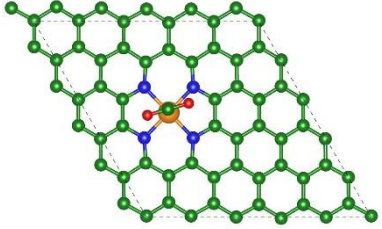
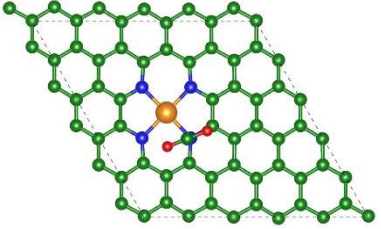
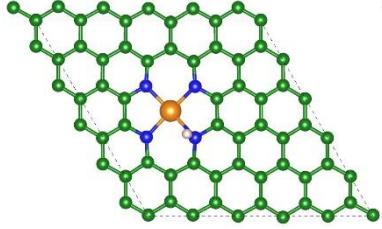
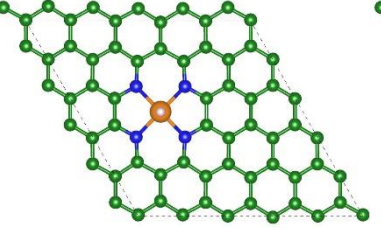
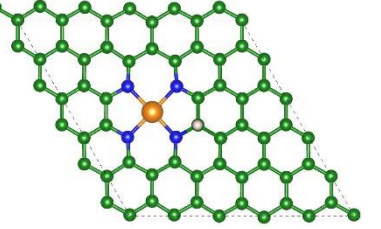
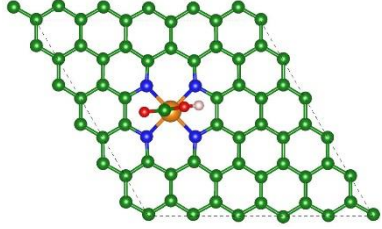
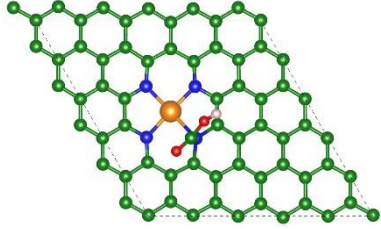
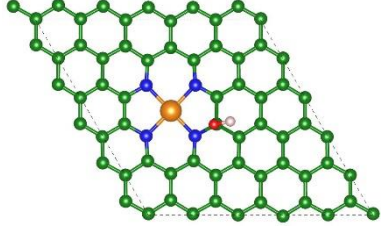
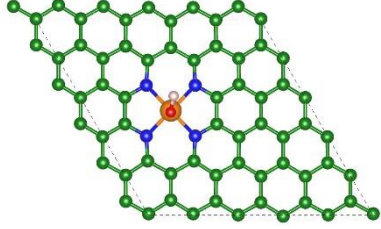
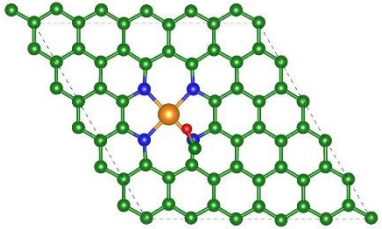
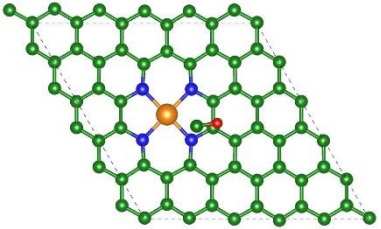
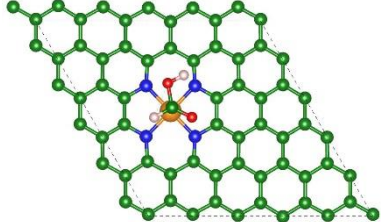
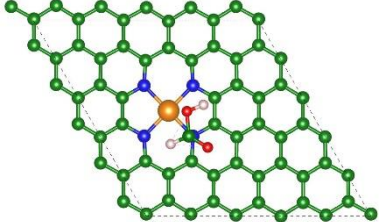
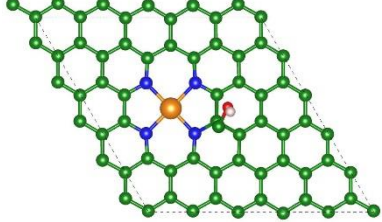
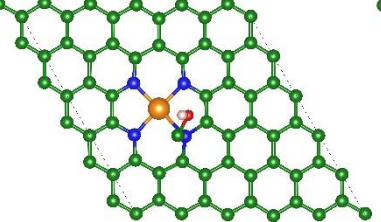
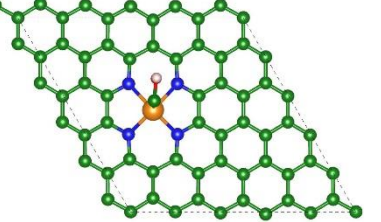
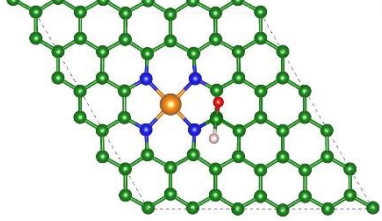
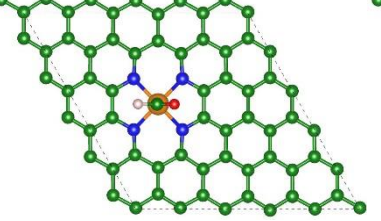
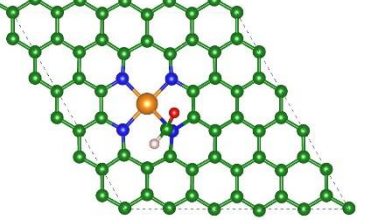
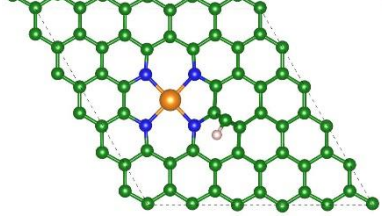
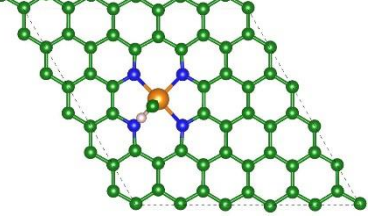
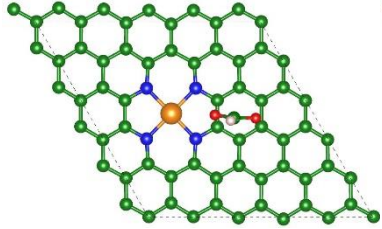
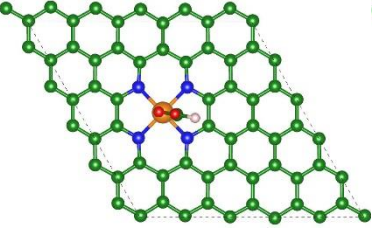
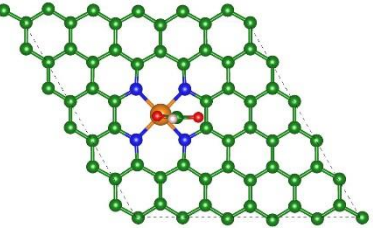
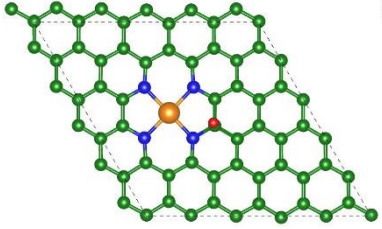
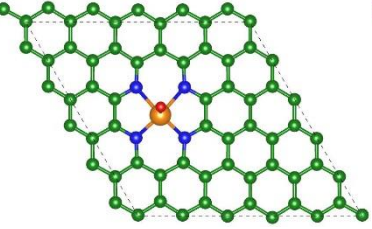
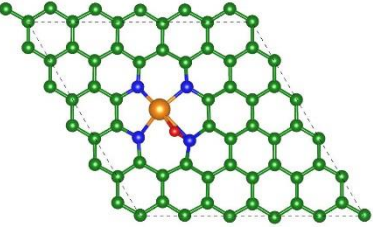
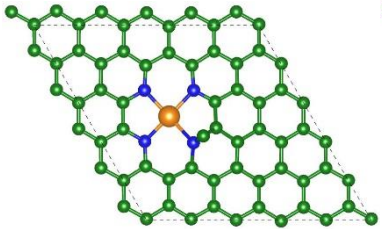
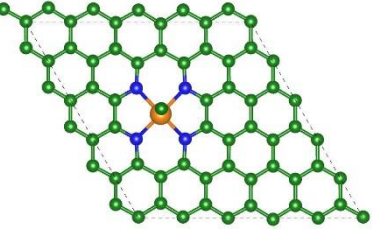
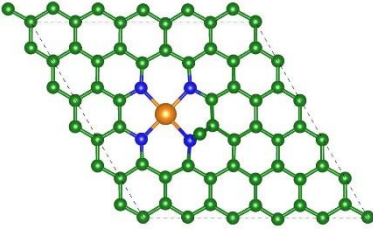
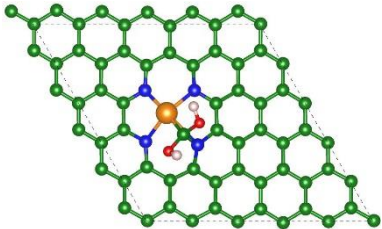
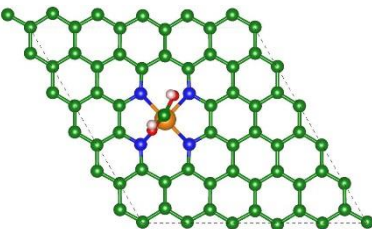
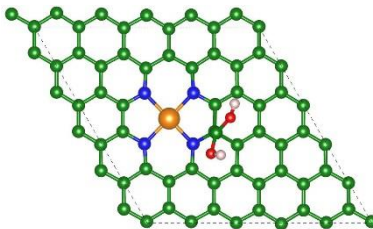
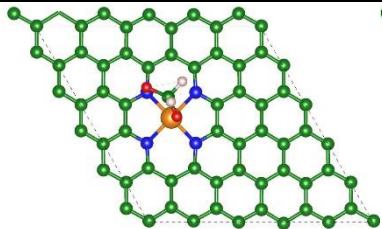
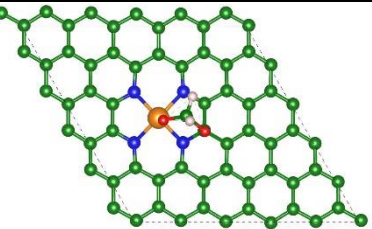
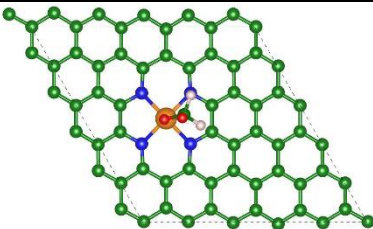
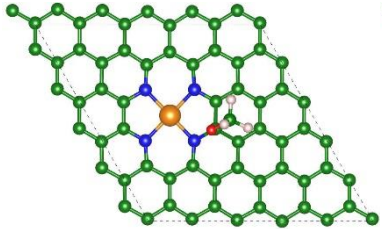
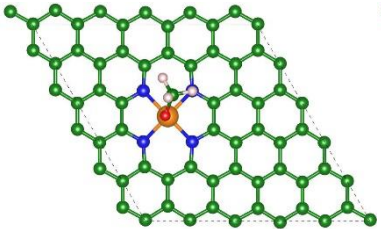
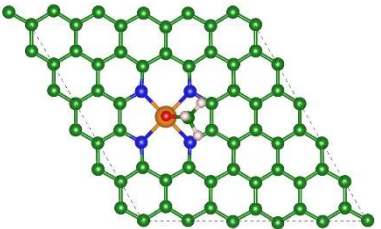
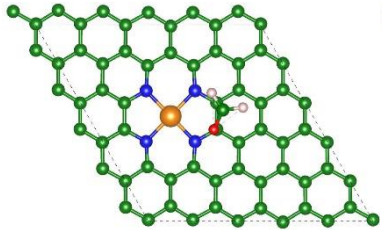
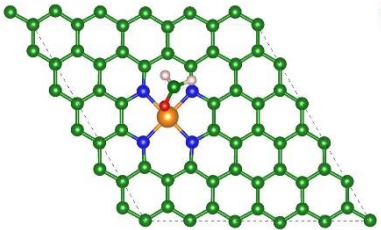
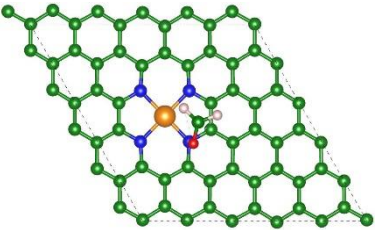
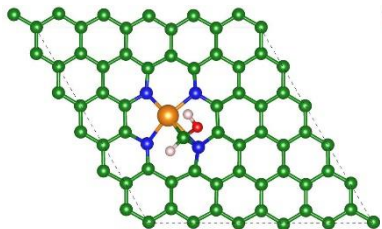
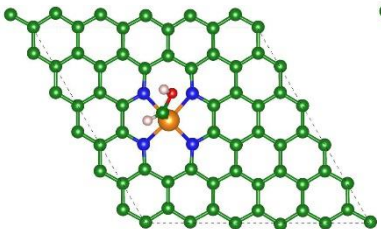
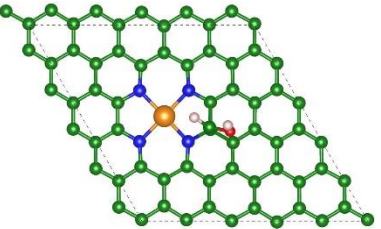
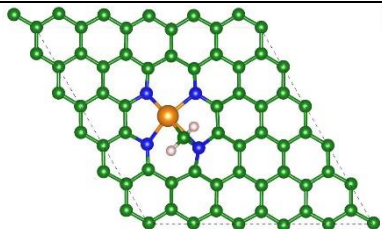
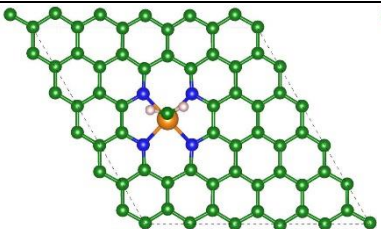
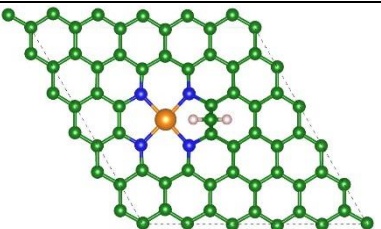
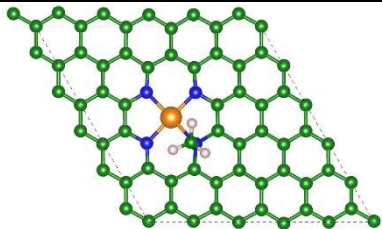
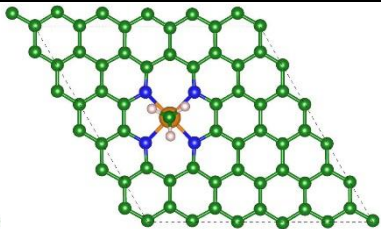
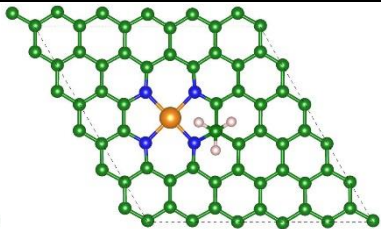
*C	 <p>3.30 4.69 4.10 4.28 4.21 4.68 3.90</p> <p>4.21 4.57 3.92 1.94</p>
*COHOH	 <p>2.85 0.52</p>
*OCH ₂ O	 <p>2.47 2.12</p>
*CH ₂	 <p>0.29 1.14</p>
*CH ₃	 <p>0.31 -0.73</p>
*CH ₂ OH	 <p>1.08</p>

Table S2 Summary of energy and configurations of possible reaction intermediates on CuNC explored by this study. Reported energies (eV) are referenced to the electronic energy of the clean Cu-C₃N₄ substrate with reference atom energies for H, C, and O obtained from ½ H₂, graphene, and (H₂O – H₂), respectively.

*CO ₂	 1.05  1.03
*H	 1.41  0.81  0.88
*COOH	 2.20  2.53
*OH	 1.54  1.47

*CO	  <p>1.83 1.82</p>
*HCOOH	  <p>0.83 0.80</p>
*COH	   <p>4.54 4.16 4.12</p>
*CHO	   <p>2.40 2.24 2.26</p>
*CH	  <p>3.98 3.33</p>

*OCHO	 2.22	 2.05	 1.76
*O	 3.10	 3.92	 3.56
*C	 5.28	 6.63	 5.28
*COHOH	 3.42	 2.64	 3.53
*OCH ₂ O	 3.80	 3.75	 3.93

*OCH₃	 1.44	 1.29	 1.28
*OCH₂	 1.15	 1.14	 1.16
*CHOH	 2.63	 2.80	 3.16
*CH₂	 1.71	 2.91	 1.77
*CH₃	 0.57	 0.61	 0.21

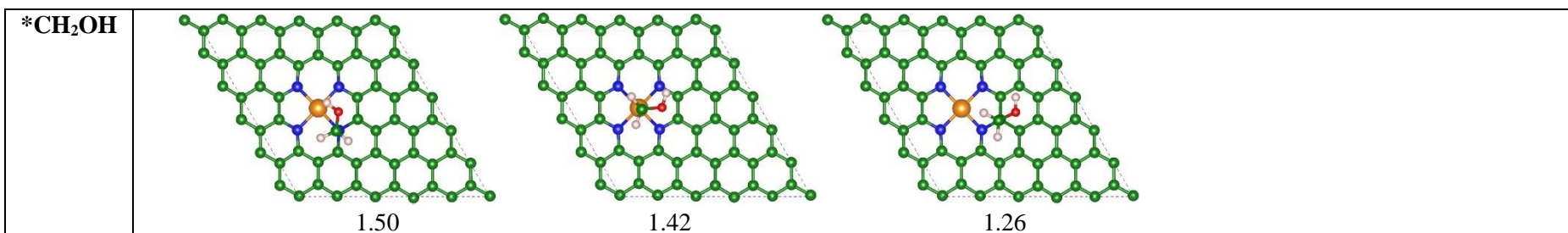


Table S3 Computed frequencies (in meV) and corresponding thermodynamic energy corrections (in eV) for selected adsorbates. Other corrections are obtained from reference [3a].

Adsorbate	ZPE	$\int C_p dT$	-TS	Frequencies
*CH ₂ O	0.76	0.10	-0.21	374.74, 362.82, 193.58, 178.69, 148.35, 114.96, 46.58, 40.08, 22.16, 18.56, 8.57, 6.39
*OCH ₃	1.15	0.08	-0.14	382.02, 376.20, 367.96, 181.36, 178.20, 175.18, 144.10, 140.62, 127.73, 76.51, 47.63, 39.16, 22.20, 16.59, 16.59

Table S4 Computed gas phase properties in eV.

Gas molecule	ZPE	$\int C_p dT$	-TS
CO	0.13	0.10	-0.61
CO ₂	0.31	0.11	-0.66
CH ₄	1.19	0.10	-0.57
C ₂ H ₄	1.35	0.11	-0.43
CH ₃ OH (g)	1.36	0.12	-0.46
HCOOH (g)	0.89	0.11	-0.50
CH ₃ CH ₂ OH (g)	2.11	0.14	-0.57

Table S5 Calculated equilibrium potentials for electrochemical CO₂ reduction for several products studied in this work.

Reaction	Equilibrium potential (vs NHE, pH = 7)
CO ₂ (g) + 2H ⁺ + 2e ⁻ → CO + H ₂ O(l)	-0.520
CO ₂ (g) + 2H ⁺ + 2e ⁻ → HCOOH(l)	-0.610
2CO ₂ (g) + 12H ⁺ + 12e ⁻ → C ₂ H ₄ + 4H ₂ O(l)	-0.359
CO ₂ (g) + 6H ⁺ + 6e ⁻ → CH ₃ OH(l) + H ₂ O(l)	-0.426
CO ₂ (g) + 8H ⁺ + 8e ⁻ → CH ₄ + 2H ₂ O(l)	-0.245
2CO ₂ (g) + 12H ⁺ + 12e ⁻ → CH ₃ CH ₂ OH (l) + 3H ₂ O(l)	-0.344

Reference

1. Cramer, C. J., *Essentials of computational chemistry : theories and models*. West Sussex, England ; New York : J. Wiley: 2002.
2. Zhu, D. D.; Liu, J. L.; Qiao, S. Z., *Adv. Mater.* **2016**, 28, 3423.
3. (a) Peterson, A. A.; Abild-Pedersen, F.; Studt, F.; Rossmeisl, J.; Norskov, J. K., *Energy Environ. Sci.* **2010**, 3, 1311; (b) Jones, G.; Jakobsen, J. G.; Shim, S. S.; Kleis, J.; Andersson, M. P.; Rossmeisl, J.; Abild-Pedersen, F.; Bligaard, T.; Helveg, S.; Hinnemann, B.; Rostrup-Nielsen, J. R.; Chorkendorff, I.; Sehested, J.; Nørskov, J. K., *J. Catal.* **2008**, 259, 147.
4. Durand, W. J.; Peterson, A. A.; Studt, F.; Abild-Pedersen, F.; Norskov, J. K., *Surf. Sci.* **2011**, 605, 1354.
5. (a) Norskov, J. K.; Rossmeisl, J.; Logadottir, A.; Lindqvist, L.; Kitchin, J. R.; Bligaard, T.; Jonsson, H., *J. Phys. Chem. B* **2004**, 108, 17886; (b) Jiao, Y.; Zheng, Y.; Jaroniec, M.; Qiao, S. Z., *J. Am. Chem. Soc.* **2014**, 136, 4394.
6. Shi, C.; Chan, K.; Yoo, J. S.; Norskov, J. K., *Org. Process Res. Dev.* **2016**, 20, 1424.